

Reversible formation of molecular junctions in two-dimensional nanoparticle arrays

Dr. Jianhui Liao¹, Laetitia Bernard¹, Michael Langer², Prof. Christian Schönenberger¹ and Dr. Michel Calame^{1}*

¹Institut für Physik, Universität Basel, Klingelbergstrasse 82, CH-4056 Basel, Switzerland

²Departement Chemie, Universität Basel, St. Johannis-Ring 19, CH-4056 Basel, Switzerland

*email: michel.calame@unibas.ch, phone: +41 61 2673697, fax: +41 61 2673784

Molecular electronics^[1] is attracting an increasing research attention, primarily supported by the possibilities offered by synthetic chemistry for the tailoring of single molecules to achieve specific electronic functions.^{[2]-[4]} Whereas various experimental approaches have been devised to form and electrically study molecular junctions,^{[5]-[11]} the integration of individual junctions into functional electronic circuits remains a demanding task, requiring innovative approaches in fabrication philosophy and circuit structure.^{[12],[13]} We show here that an approach combining the self-assembly^[14] and micro-contact printing^[15] of ligand-protected metallic nanoparticles, followed by an *in-situ* ligand exchange reaction,^[16] allows the preparation of stable two-dimensional networks of molecular junctions.^[17] A significant decrease in resistance (up to three order of magnitude) after the exchange of alkanethiols ligands with conjugated, double-ended organic wires (thiolated oligo(phenylene ethynylene), OPE) confirms a proper interlinking of neighbouring nanoparticles. We also demonstrate that the formation of the molecular junctions is reversible, making nanoparticle networks a promising platform for the development of molecular electronic circuits. The flexibility of this approach lets envision the realisation of more complex networks, for instance by intermixing ensembles of bimodal nanoparticles^[18] of different materials.

Both experimental and theoretical evidence show that the electronic properties of molecular junctions are not only dictated by the molecules contacted but also depend on the anchoring groups and the electrodes forming the junction.^{[3],[11]} The use of nanometer-size metallic colloids as electrodes appears therefore as an elegant solution to build molecular junctions with well-defined geometry and electronic properties. Recent results on colloid dimers interlinked by a conjugated molecule demonstrate the validity of this approach.^[19] The demonstration here of the fabrication of reversible two-dimensional networks of hybrid metallic colloid-organic molecule junctions, opens new possibilities for the realization of molecular circuits.

Alkanethiol-capped 10nm gold nanoparticles were first self-assembled into two-dimensional (2D) close-packed arrays at the air/water interface.^[20] A polydimethylsiloxane (PDMS) stamp with the desired imprinted structures was then prepared to print patterned nanoparticle monolayers on a solid substrate.^[15] Figure 1a shows a scanning electron micrograph (SEM) image of dodecanethiol-capped nanoparticle monolayer lines printed with a PDMS stamp on a SiO₂/Si substrate. The lines have a typical width of 25μm and a spacing of 30μm. In contrast to other approaches for the preparation of interlinked nanoparticle arrays, such as layer-by-layer assembly,^[21] Langmuir-Blodgett technique,^[22] and multiple deposition on solid substrates,^{[23],[24]} the stamping technique yields spatially well positioned arrays (Fig.1a, c), free of multilayer regions (Fig.1b). High magnification SEM images (Fig.1d-f) reveal that the nanoparticles are well separated from each other by the alkanethiol chains and order in a hexagonal close-packed structure. The inter-particle distance can be increased by using alkanethiols with increasing lengths as shown by the SEM images of nanoparticle arrays prepared with octanethiol (C8), dodecanethiol (C12) and hexadecanethiol (C16) ligands (Fig1d, -e and -f, respectively).

The stamped nanoparticle arrays remain stable for several weeks in air at room temperature without showing aggregation and can resist common solvents, such as tetrahydrofuran (THF), ethanol, or toluene. This good mechanical and chemical stability enables us to use the nanoparticles arrays as a “colloidal breadboard” to fabricate networks of molecular junctions.

To investigate the electrical transport through the patterned nanoparticle arrays, contact pads (5nm Ti + 45nm Au thick) were deposited on top of the printed monolayer lines using a transmission electron microscope (TEM) grid as a shadow mask. Figure 2a shows a SEM image of a typical device composed of two square-shaped contact pads evaporated on a line of octanethiol-encapsulated nanoparticles. The rectangular particles array between two contact pads is typically 12 μ m in length (l) by 25 μ m in width (w). According to SEM inspection, the arrays are kept intact, with no noticeable change of the structures observed after evaporation of the contact pads.

The electrical measurements of the devices were performed on a probe station in air at room temperature. For the comparison of various devices, we will consider the sheet resistance $R_{\square} = R \cdot w/l$, where R is the measured resistance of an array, with l and w the length and width defined as in Fig. 2a. Figure 2b shows typical DC I-V curves of a device measured at four steps in the course of a molecular exchange experiment. Curve 1 (black) shows the electronic behaviour of an as-prepared device (C8 ligands) with sheet resistance $R_{\square 1} = 4.4 \times 10^{10} \Omega$. The device was then immersed in a 1mM OPE solution in THF for 24 hours, followed by a 10min rinse in THF. The sheet resistance after OPE exchange (curve 2, red) was found to be $R_{\square 2} = 6.3 \times 10^7 \Omega$, a decrease by more than two orders of magnitude.

A maximum bias voltage of 10V was applied to the device, yielding a maximum voltage drop over one molecular junction of 10mV, since the device is formed by about one thousand junctions in series. This value is lower than the thermal energy $k_B T$, amounting to 26meV at room temperature, and therefore ensures a linear response of the device. In addition the single electron charging energy of individual nanoparticles is estimated to be smaller than $k_B T$.

We attribute the significant decrease of resistance observed between curves 1 and 2 to the formation of interlinked molecular junctions by the dithiolated OPE molecules. In the as-prepared device, nanoparticles are separated by octanethiol molecules, as shown by the schematic drawing in Fig.2c (left). From The average edge to edge distance of neighboring particles was found to be about 2.4nm, very close to the S-S length of the OPE molecule (~ 2.1 nm). It has been demonstrated that alkanethiolate monolayer-protected gold clusters can be functionalized by introducing new thiolate

ligands through a place-exchange reaction.^[16] During the device immersion in the OPE solution, the incoming organic molecules can penetrate the octanethiol monolayer and bind to the nanoparticle. For molecules with two anchoring groups, neighboring nanoparticles have a significant chance to be interlinked, thereby forming a network of molecular junctions. This process is schematically represented in Fig.2c. OPE being a conjugated compound and, therefore, a better electron carrier than alkanethiols, the resistance of OPE interlinked array is expected to be smaller than that of unlinked arrays. This is true as long as the contacts (the thiol linkers) provide a sufficient electronic coupling of the molecule with the colloids. A SEM inspection of the devices before and after OPE exchange revealed that the morphology and general structure of the nanoparticle array remain unchanged during the exchange process as shown in Fig.2d. The gold nanoparticles array forms a robust nanoelectrode skeleton, a “colloidal breadboard”. Control experiments show that devices immersed in pure THF, without OPE molecules, do not substantially change their resistance. We also measured that the resistance between two contact pads without a nanoparticle array is above $10T\Omega$, both before and after OPE treatment. We are therefore confident that the significant change of resistance observed can be attributed to the interlinking of neighbouring nanoparticles by the OPE molecules.

Remarkably, the formation of molecular junctions has been found to be *reversible*. After the OPE exchange described above, we immersed the same device for 24h in a 0.5M octanethiol solution in THF, followed by a 24h immersion in a pure octanethiol solution. The DC I-V curve (curve 3, black) of the device after this treatment showed a similar behaviour as that of the as-prepared device. The sheet resistance was measured to be $R_{\square 3} = 5.4 \times 10^{10} \Omega$, indicating that OPE molecules had been replaced by octanethiols. A second OPE exchange (curve 4, red), following the above described procedure, caused the sheet resistance to drop to $R_{\square 4} = 7.2 \times 10^7 \Omega$, a similar value to that obtained after the first OPE exchange ($6.3 \times 10^7 \Omega$).

Fig.2e shows the evolution of the sheet resistance of a device immersed in a 1 mM OPE solution in THF at different times during the exchange process (the device was rinsed and dried before each measurement). We observe that the sheet resistance decreases rapidly in the first 40 minutes and then

saturates. This is consistent with the results of Murray *et al.*,^[16] who determined the rate of place-exchange on monolayer-protected clusters.

The stamping technique permits the simultaneous preparation of hundreds of devices on a single chip, an essential asset for the characterization of molecular devices. Figure 3a presents the sheet resistance of twenty-nine devices selected randomly on one chip during two successive cycles of molecular exchange: all devices exhibit the same behavior. The average sheet resistances measured at various stages, namely (i) as-prepared, (ii) after a first OPE exchange, (iii) after an octanethiol exchange, and (iv) after a second OPE exchange, were respectively $3.8 \times 10^{10} \Omega$, $6.4 \times 10^7 \Omega$, $5.2 \times 10^{10} \Omega$, and $6.5 \times 10^7 \Omega$. These data show the high yield and very good reproducibility of the reversible formation of molecular junctions.

In Figure 3b, we summarize the results obtained from one hundred devices measured on five *different* chips. We show here the sheet resistance of each device before (black) and after (red) OPE exchange. It is clear that, no matter what the resistance is before exchange, the resistance of the interlinked arrays is around a few tens of $M\Omega$ for most devices, after exchange. We attribute the chip-to-chip resistance differences of the as-prepared devices (black) to variations in the average inter-particle distance. Different surface pressures during the arrays self-assembly at the air/water interface can lead to this effect, as also observed by Heath *et al.*^[25] After exchange (red), we observe a remarkable attenuation of these variations, showing that the OPE molecules can (at least partially) overcome a distribution of inter-colloid distances by self-adjusting within the gap. This also points towards a real inter-linking mechanism rather than an intermolecular charge transport due to the possible overlap of OPE's linked to neighboring nanoparticles, although the latter cannot be excluded. We obtain values of R_{\square} ranging typically between 10 $M\Omega$ and 100 $M\Omega$, yielding an average value (over the hundred devices) of $R_{\square} \approx 54 M\Omega$.

We may model an array as a hexagonal network of nodes interconnected by identical classical resistors R_J . The sheet resistance of the network R_{\square} is then related to the junction resistance R_J by $R_{\square} = (\sqrt{3}/2) \cdot R_J$. The average resistance of a junction formed by two OPE-interlinked colloids

corresponds therefore to a value of $R_J \approx 62 \text{ M}\Omega$. Recent STM experiments have provided a value of $77 \text{ M}\Omega$ for the resistance of a *single* OPE molecule,^[26] which is very close to the junction resistance R_J in the present work. This finding translates to an average of ~ 1.2 molecules per junction in our arrays. The self-adjustability does therefore not only reduce the spread in R_{\square} after the assembly of dithiolated OPEs, but we also observe that this mechanism favours the self-formation of single molecular junctions, an asset for producing robust building blocks in molecular electronics.

In conclusion, we have demonstrated the reversible formation of molecular junction networks using a molecular exchange technique in two-dimensional metallic nanoparticle arrays. The stability, high yield, and reproducibility of the devices shall establish this method as a promising tool for the development of molecular circuits. Functional molecular devices might be fabricated by assembling hybrid structures composed of nanoparticles (metallic or semiconducting) linked by conducting wires and electro- or photo-active molecules.

ACKNOWLEDGMENTS We gratefully acknowledge fruitful discussions with M.A Ratner. This work benefited from the support of the Swiss National Center of Competence in Research “Nanoscale Science”, the Swiss National Science Foundation and the European Science Foundation through the Eurocores Programme on Self-Organized Nano-Structures.

EXPERIMENTAL

Gold colloidal particles with a diameter of 10nm were synthesized using the method described by Slot et al.^[27] Unless mentioned, all reagents were purchased from Fluka and used as received. A 20ml solution containing 4ml 1%(w/v) trisodium citrate and 0.08ml 1% tannic acid was rapidly added to an 80ml solution containing 1ml 1%(w/v) chloroauric acid (all solutions at 60°C). The mixed solution was boiled for 10 minutes while continuously stirring and then cooled down to room temperature with chilled water.

The encapsulation of the gold nanoparticles with alkanethiols was performed following the procedures described by Huang et al.^[28] The nanoparticles were first transferred from water to ethanol by centrifugation and mixed together with a 0.5M solution of alkanethiols in ethanol. After 12h, the nanoparticles were properly capped with alkanethiols and precipitated at the bottom of the container. The precipitates were washed with ethanol in order to remove excess alkanethiols. Finally, the alkanethiol-capped nanoparticles were dispersed in chloroform by ultrasonic treatment.

Two-dimensional arrays of nanoparticles were prepared by self-assembly at an air/water interface.^[15] In a typical experiment, 400 μ l of $\sim 2 \times 10^{13}$ particles/ml alkanethiol-encapsulated gold nanoparticles dissolved in chloroform were cast with a syringe at the air/water interface of a Teflon container filled with pure, deionized water. The shape of the water surface was adjusted to be slightly convex. After evaporation of the solvent (fume hood, air velocity at 100 ft/s), the nanoparticles self-assembled into a two-dimensional array at the water surface.

The polydimethylsiloxane (PDMS) stamps were prepared by casting a mixture of a pre-polymer gel and a curing agent (Sylgard 184, Corning) on a master having the desired patterns. After degassing at room temperature for 30min and baking at 60°C for 1-2h, the PDMS stamps were peeled off the master and cut into the desired shape.

A 1mM solution of OPE in THF was used for the molecular exchange of octanethiol with the OPE molecules. Samples were immersed in 2mL of the OPE solution for more than 20 hours. The solution was bubbled with Ar before immersion of the samples and kept under Ar during the exchange process. After exchange, the samples were rinsed in THF to remove the unreacted materials and dried with nitrogen gas.

Figure 1 Electron microscope images of alkanethiol-capped gold nanoparticles ($\text{\O} 10\text{nm}$) on a SiO_2/Si substrate. **a**, The particles were self-assembled at an air/water interface and transferred to the substrate with a PDMS stamp to form parallel lines of nanoparticles monolayers. The higher magnification images show: **b**, the dense packing of the array and **c**, the well-defined edges. Detailed views ($100\text{nm}\times 100\text{nm}$) of nanoparticles arrays stabilized with **d**, octanethiol, **e**, dodecanethiol and **f**, hexadecanethiol ligands, reveal a hexagonal close-packed ordering. For the longer chain lengths, the ordering improves and the inter-particle spacing increases.

Figure 2 Transport measurements through a colloid array before and after molecular exchange. **a**, electron microscope image of a device: two square-shaped gold contacts were evaporated on top of a nanoparticle array line of width w . **b**, Typical I-V curves measured at different stages in a molecular exchange experiment: 1: as-prepared octanethiol array; 2: after OPE exchange (first time); 3: after octanethiol exchange; 4: after OPE exchange (second time). Inset: curves 1 and 2 shown at lower current values. **c**, Schematic of the molecular exchange process. *Left*: self-assembled alkanethiol-capped nanoparticles before exchange; *right*: during the exchange process, the OPE molecules (red) displace part of the alkane chains and interlink neighbouring nanoparticles to form a network of molecular junctions. **d**, Electron microscope images of the array structure before and after OPE exchange. **e**, Resistance change of a device as a function of immersion time in the OPE solution during the course of molecular exchange (from stage 1 to 2).

Figure 3 Reproducibility of the exchange process. **a**, Sheet resistance of 29 nanoparticle arrays on one chip. The sheet resistance of each octanethiol device was measured “as-prepared” (■) and after a first exchange with the OPE molecules (●). A subsequent exchange with octanethiols reversed the devices to their initial state (△) and a second exchange with OPEs proved the full reversibility of the process (▽). The bottom left inset is an electron microscope picture of devices fabricated by evaporation of gold contact pads on nanoparticle monolayer lines. Scale bar: 50μm. **b**, Sheet resistance of one hundred devices on five *different* chips (■,○,▲,▽,◆) measured before (black symbols) and after OPE exchange (red symbols). The horizontal dashes show the average sheet resistance values. The large sheet resistance differences between chips in the as-prepared devices are strongly reduced after molecular exchange.

REFERENCES

- [1] J.R. Heath, M.A. Ratner, *Physics Today* **2003**, *56*, 43.
- [2] A. Aviram, M.A. Ratner, *Chem. Phys. Lett.* **1974**, *29*, 277.
- [3] A. Nitzan, M.A. Ratner, *Science* **2003**, *300*, 1384.
- [4] C. Joachim, J.K. Gimzewski, A. Aviram, *Nature* **2000**, *408*, 541.
- [5] M.A. Reed, C. Zhou, C.J. Muller, T.P. Burgin, J.M. Tour, *Science* **1997**, *278*, 252.
- [6] W. Liang, M. P. Shores, M. Bockrath, J.R. Long, H. Park., *Nature* **2002**, *417*, 725.
- [7] B. Xu, N. Tao, *Science* **2003**, *301*, 1221.
- [8] J. Chen, M.A. Reed, A.M. Rawlett, J.M. Tour, *Science* **1999**, *286*, 1550.
- [9] J.G. Kushmerick, D.B. Holt, J.C. Yang, J. Naciri, M.H. Moore, R. Shashidar, *Phys. Rev. Lett.* **2002**, *89*, 086802.
- [10] R.E. Holmlin, R. Haag, M.L. Chabinyc, R.F. Ismagilov, A.E. Cohen, A. Terfort, M.A. Rampi, G.M. Whitesides, *J. Am. Chem. Soc.* **2001**, *123*, 5075.
- [11] R.L. McCreery, *Chem. Mater.* **2004**, *16*, 4477.
- [12] J. R. Heath, P.J. Kuekes, G.S. Snider, R.S. Williams, *Science* **1998**, *280*, 1716.
- [13] Y. Chen, G.-Y. Jung, D.A.A. Ohlberg, X. Li, D.R. Stewart, J.O. Jeppesen, K.A. Nielsen, J. Fraser-Stoddart, R.S. Williams, *Nanotechnology* **2003**, *14*, 462.
- [14] G.M. Whitesides, B. Grzybowski, *Science* **2002**, *295*, 2418.
- [15] V. Santhanam, R.P. Andres, *Nano Letters* **2004**, *4*, 41.
- [16] M. J. Hostetler, A.C. Templeton, R.W. Murray, *Langmuir* **1999**, *15*, 3782.

- [17] S. Datta, *Semicond. Sci. Technol.* **1998**, *13*, 1347.
- [18] C.J. Kiely, J. Fink, M. Brust, D. Bethell, D.J. Schiffrin, *Nature* **1998**, *396*, 444.
- [19] T. Dadosh, Y. Godrin, R. Krahn, I. Khivrich, D. Mahalu, V. Frydman, J. Sperling, A. Yacobi, I. Bar-Joseph, *Nature* **2005**, *436*, 677.
- [20] V. Santhanam, J. Liu, R. Agarwal, R.P. Andres, *Langmuir* **2003**, *19*, 7881.
- [21] J.M. Wessels, H.-G. Nothofer, W.E. Ford, F. von Wrochem, F. Scholz, T. Vossmeier, A. Schroedter, H. Veller, A. Yasuda, *J. Am. Chem. Soc.* **2004**, *126*, 3349.
- [22] S. Chen, *Langmuir* **2001**, *17*, 2878.
- [23] D.B. Janes, V.R. Kolagunta, R.G. Osifchin, J.D. Bielefeld, R.P. Andres, J.I. Henderson, C.P. Kubiak, *Superlattices and Microstructures* **1995**, *18*, 275.
- [24] R.P. Andres, J.D. Bielefeld, J.I. Henderson, D.B. Janes, V.R. Kolagunta, C.P. Kubiak, W.J. Mahoney, R.G. Osifchin, *Science* **1996**, *273*, 1690.
- [25] See e.g. J.F. Sampaio, K.C. Berberly, J.R. Heath, *J. Phys. Chem. B* **2001**, *105*, 8797 and references therein.
- [26] X. Xiao, L.A. Nagahara, A.M. Rawlett, N.J. Tao, *J. Am. Chem. Soc.* **2005**, *127*, 9235.
- [27] J.W. Slot, H.J. Geuze, *Eur. J. Cell Biol.* **1985**, *38*, 87.
- [28] S. Huang, G. Tsutsui, H. Sakaue, S. Shingubara, T. Takahagi, *J. Vac. Sci. Technol. B* **2001**, *19*, 115.

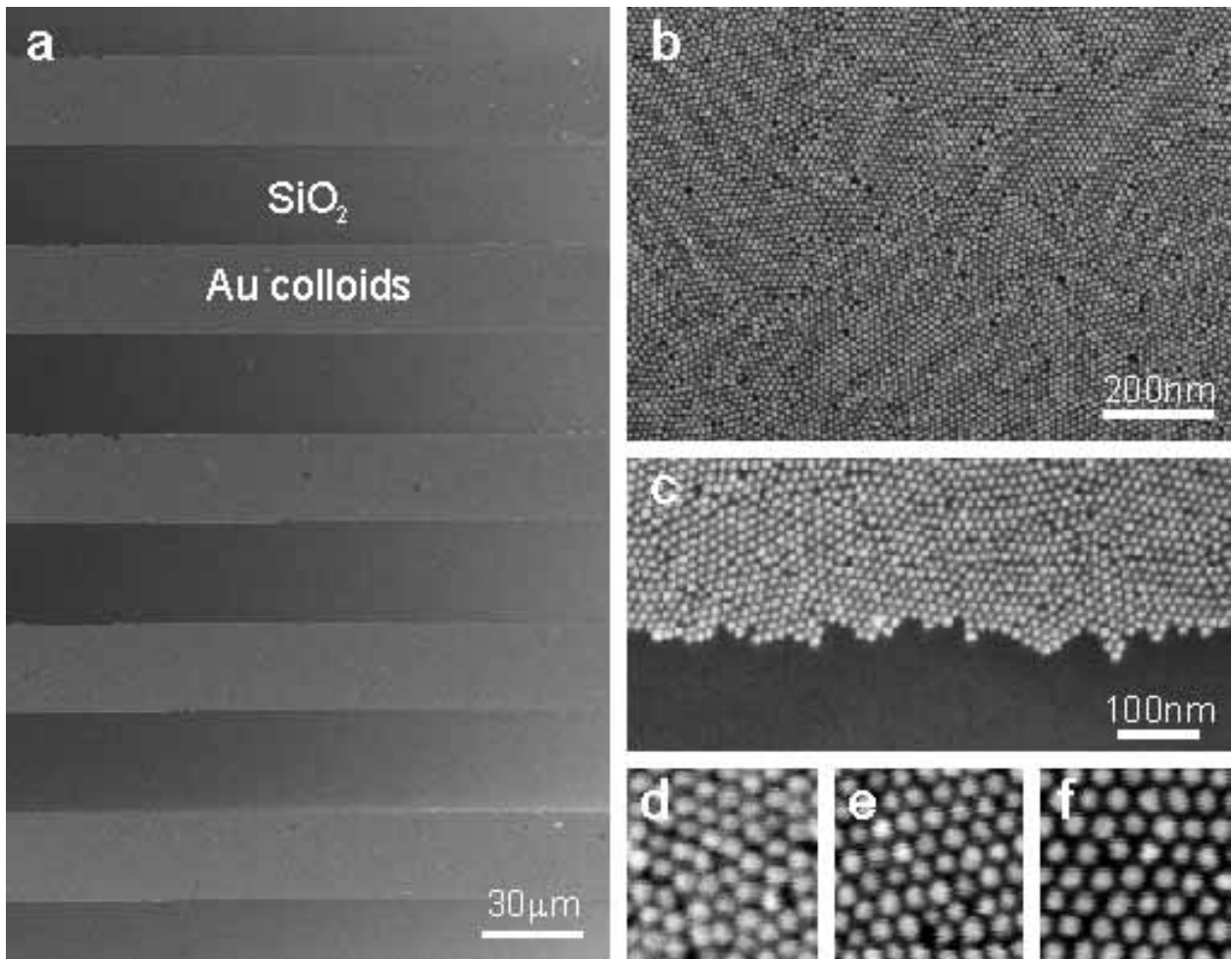


Figure 1

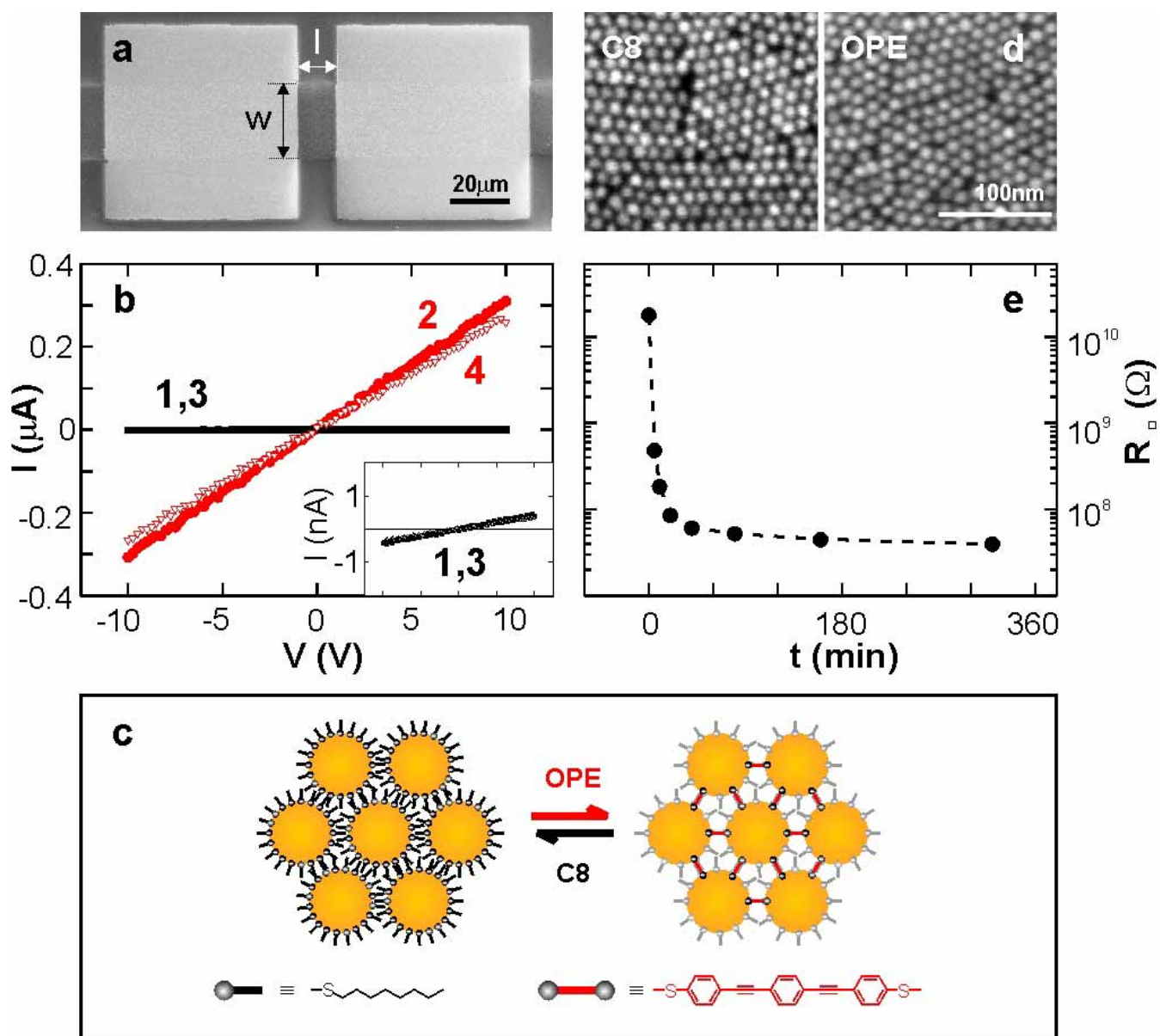


Figure 2

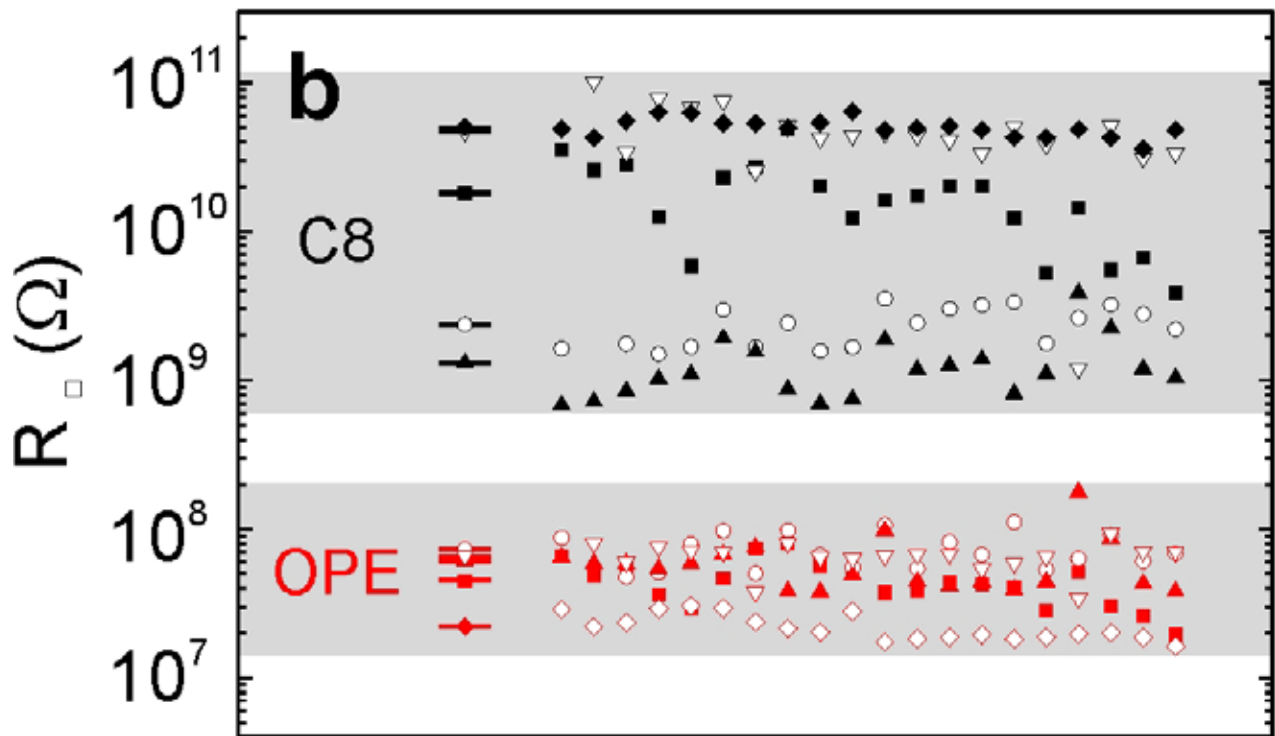
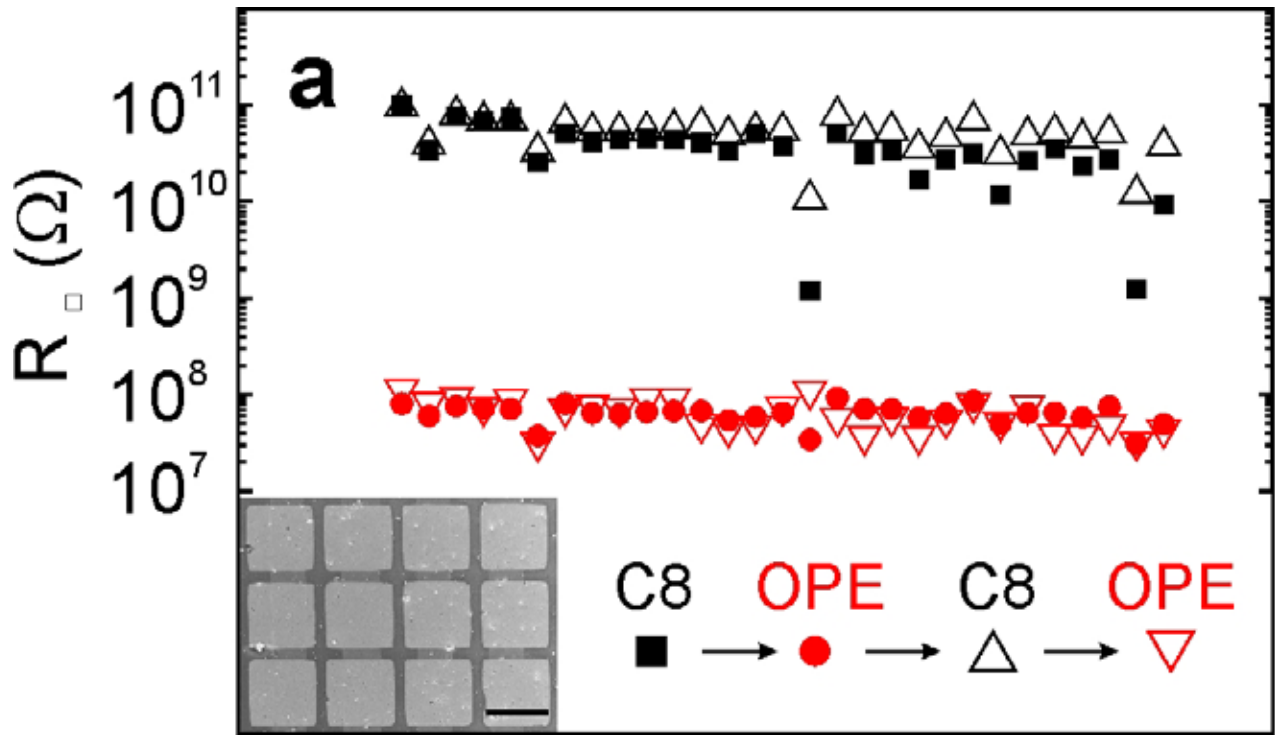


Figure 3